(Received 26 October 2023, Accepted 26 December 2023, Scheduled 9 January 2024)

Low-Cost High Gain Sea Pimp-Shaped Dual Band Monopole Antenna for Mobile 4G/5G/LTE41/WLAN Application

Suwat Sakulchat[1], Amnoiy Ruengwaree[2,*], Watcharaphon Naktong[3,*], Pramuk Unahalekhaka[4], and Sommart Promput[5]

[1]*Department of Electrical Engineering, Faculty of Engineering and Architecture Rajamangala University of Technology Suvarnabhumi, Phranakhon Si Ayutthaya 13000, Thailand*
[2]*Department of Electronics and Telecommunication Engineering, Faculty of Engineering Rajamangala University of Technology Thanyaburi, Pathum Thani 12110, Thailand*
[3]*Department of Telecommunications Engineering, Faculty of Engineering and Technology Rajamangala University of Technology Isan, Nakhon Ratchasima 30000, Thailand*
[4]*Department of Electrical Engineering, Faculty of Engineering and Architecture Rajamangala University of Technology Suvarnabhumi, Nonthaburi 11000, Thailand*
[5]*Department of Mechatronics and Robotics Engineering, School of Engineering and Innovation Rajamangala University of Technology Tawan-ok, Chonburi 20110, Thailand*

ABSTRACT: This research aimed to design a sea pimp-shaped monopole antenna by using etching and cutting techniques, combined with the addition of reflector, to modify the antenna structure to support the bandwidth standard according to GSM-850 (0.82–0.90 GHz), GSM-900 (0.88–0.96 GHz), DCS (1.72–1.88 GHz), PCS (1.85–1.99 GHz), UMTS (1.92–2.17 GHz), 5G Band40 (2.30–2.40 GHz), LTE41 (2.496–2.690 GHz), and WLAN IEEE 802.11b/g/n (2.4–2.48 GHz). This antenna used a galvanized metal sheet with a conductivity of 3.56×10^7 s/m to fabricate the structure of the radiator, ground plane, and reflector. The reflector modifies radiation patterns and increases the gain of the antenna. The antenna structure used the CST program for simulation to determine the optimal parameters and property values. As a result of replication, the antenna had dual bands with a reflection coefficient (S_{11}) at 915 MHz (736–1040 MHz) of -26.70 dB and a frequency at 2.28 GHz (1.68–2.94 GHz) of -20.15 dB. The antenna gains are 6.70 and 8.47 dBi, an increase of 83.56% and 44.04% over the antenna without a reflector, respectively. The antenna had a unidirectional pattern in all the frequency ranges which can be utilized for the purpose of RF energy-harvesting (RF-EH) systems to provide power to low-power electronic systems.

1. INTRODUCTION

The cellular communication system has evolved from the 1G (First Generation) era, where cellular signal transmission was analog, in which radio signals were transmitted over voice signals only. Later, it was upgraded to the 2G era (by changing it from analog transmission to digital encoding transmitted by microwave signals), which is a GSM (Global System for Mobile Communications) mobile phone system technology. However, the system still had some disadvantages regarding the loss caused by sending out a small amount of data each time. Therefore, it was developed further into the 2.5G era or GPRS (General Packet Radio Service). This service can transmit data via a mobile phone by encoding and compressing the audio in digital format. Two methods were used for transmitting data: TDMA (Time Division Multiple Access) and CDMA (Code Division Multiple Access). The system was further developed into the 2.75G era when the technology began EDGE (Enhanced Data Rates for Global Evolution). This technology works when the phone is in use and is allocated to each phone to be used within the same frequency channel. 3G is the third generation of data transmission in wireless systems, with higher speed rates and more capacity frequency channels. This network system is commonly used for communication devices. Mobile phones, computers, iPads, tablets, and laptops are necessary for everyday life, mainly by providing multimedia services, including audio and animation data, with WCDMA (Wideband Code Division Multiple Access) technologies [1–5].

The current system, the 4G era, has further developed data transmission speed and network connection with the IP protocol into one technology. The primary service of the mobile phone system is the use of LTE (Lone Term Evolution) technology [6–8]. LTE has the advantage of increasing the frequency range mainly by enabling applications to continuously run on the internet network (such as watching TV programs on mobile phones, loading movies, having a teleconference, saving travel budgets, or organizing meetings that are otherwise very expensive today). Recently, 4G has evolved into 5G applications, which will be able to provide fast big data transmission services and applied in various intelligent technology applications [9].

Wireless communication is commonly used in the frequency bands that comply with IEEE standards (namely IEEE 802.11b/g/n in the 2.4–2.484 GHz and IEEE 802.16a/e/j in 3.4–3.69 GHz, 5.15–5.35 GHz, and 5.725–5.825 GHz) [10–15]. Wireless is used for data communication applications that require fast speed and a large amount of information,

* Corresponding authors: Amnoiy Ruengwaree (amnoiy.r@en.rmutt.ac.th); Watcharaphon Naktong (watcharaphon.na@rmuti.ac.th).

which results from implementing such applications. The antenna is an essential component of a transmission system. Numerous research studies have focused on designing and developing antennas to have better performance in terms of response and multi-band support, as well as to have a high gain on a single basic antenna structure that covers both mobile and WLAN due to its simple design. In a previous study, a monopole antenna with circular shape laid parallel on top of rectangular ground plane was studied. The antenna used a strip line to feed the signal into the radiator to cover a wideband of frequencies at 2.69–10.16 GHz for ultra-wideband (UWB) with an average gain of 3.5–6.7 dBi [16]. A monopole antenna with a circular structure perpendicular to a square-shaped ground plane covering 0.4–4 GHz was found to support RFID and GPS applications with an average gain of 5–8 dBi [17]. A circular monopole antenna was designed with a spiral shape perpendicular to a square-shaped ground plane to support the use in 3.1–10.6 GHz range for UWB signal plus systems [18]. In [19], it was found that four circular discs are joined in a cross-shaped way, perpendicular to the circular ground plane, which supports the frequency range in UWB from 4.00 GHz to 15.00 GHz, with an average gain of 5.7–8.1 dBi. Four L-shaped ellipse antennas were designed to cross perpendicular to the circular ground plane with two circular grooves inside to support dual bands at 1.69–3.15 GHz and 4.93–6.62 GHz in WLAN, GSM, UMTS, and LTE systems, with an average gain of 3.1–5.1 dBi [20]. A circular monopole antenna was placed on top of the same plane as the ground plane to support dual-band applications of 0.82–1.25 GHz and 1.65–2.79 GHz in GSM, CDMA, and WLAN and had an average gain of 3.7 dBi [21]. A circular monopole antenna was designed on an FR-4 substrate, which had a ground plane overlaid below by feeding the signal through the strip line to cover the frequency range of 1.48–35 GHz that supported the UWB with an average gain of 2.5–5.25 dBi [22]. As mentioned above, the design has a lot of complexity. In addition, in the frequency range used in the GSM-850 (0.82–0.90 GHz) and GSM-900 (0.88–0.96 GHz) ranges, there is still a value in the range of 3–5 dBi, which is not very high and makes it possible to test for actual use, which may affect the distance in receiving and sending signals that are not very far. Furthermore, in the GSM-850 (0.82–0.90 GHz) and GSM-900 (0.88–0.96 GHz) frequency ranges, there is still a low value in the range of 3–5 dBi, which makes it possible to test for actual use and may affect the distance in receiving and sending signals that are not very far.

A low-cost circular monopole antenna structure with a galvanized metal sheet was the goal of this study [21]. It was to support the standard frequency bands GSM-850 (0.82–0.90 GHz), GSM-900 (0.88–0.96 GHz), DCS (1.72–1.88 GHz), PCS (1.85–1.99 GHz), UMTS (1.92–2.17 GHz), and WLAN band IEEE 802.11b/g/n (2.4–2.48 GHz) [21]. This antenna was designed by cutting only two rectangular grooves until the antenna resembled a sea pimp shape [23–24] and using the reflector technique to increase antenna gain [25–27]. The CST program assisted in antenna simulation, factoring the reflection coefficient (S_{11}), bandwidth, radiation pattern, and antenna gain. The antenna simulations were analyzed using the experiential method to obtain an optimal and efficient antenna.

2. ANTENNA DESIGN AND SIMULATION

This research selected a typical circular antenna [16–22] and improved that antenna structure fabricated from galvanized metal sheet with a thickness of $t_1 = 0.3$ mm because the antenna structure is readily cuttable, inexpensive, and rust-resistant. There were four steps in the antenna structure design process. The first step was designing the resonance frequency $f_r = 900$ MHz, the middle-frequency value between GSM-850 and GSM-900, which can be calculated from Equation (1) [28].

$$r_1 = \frac{0.64\lambda_c}{\pi}; \quad \lambda_c = \frac{c}{f_r} \tag{1}$$

where c = velocity of the light (3×10^8 m/s); f_r = resonance frequency; λ_c = wavelength; r_1 = radius of the radiator.

The outcome of the calculation was that the radius (r_1) of the circular monopole antenna was 68 mm. The CST program simulated a circular monopole antenna structure with a calculated parameter (Equation (1)). The center of the radiator is perpendicular to the ground plane [17–20] on galvanized metal material with a thickness (t_2) of 0.3 mm, width (W_1) adjustments of 140, 160, and 180 mm, and length (L_1) adjustments of 100, 105, and 110 mm. The signal was fed via a hole at the center of the ground plane to the bottom of the circular radiator by the feed line, with a width (W_2) of 3.1 mm and a length (L_2) of 4 mm as the most suitable parameters (Figure 1). The S_{11} of the circular antenna (the ground plane: parameters of $W_1 = 160$ mm and $L_1 = 105$ mm) was less than -10 dB at the low resonance frequency of 0.914 GHz (0.639–1.236 GHz), resulting in -29.51 dB and -22.82 dB at the high resonant frequency of 1.617 GHz (1.368–3.302 GHz), as shown in Figure 2. The radiation pattern is shown in Figure 3, where the direction of the radiation pattern was omnidirectional at the low and high resonant frequencies, with the antenna gains being 3.65 and 5.88 dBi, respectively.

Antenna tuning in the second step consists of adding a rear reflector parallel to the antenna to function as a mirror and direct the signal toward the front of the antenna [25–27]. Then, the restructured antenna was simulated with structure details as follows: The reflector is aluminum with a thickness (t_3) of 0.3 mm, width (W_3) adjustments of 220, 240, and 260 mm, and length (L_3) adjustments of 220, 240, and 260 mm. It is placed perpendicular to the ground plane and behind the radiator, with the span distance between the radiator and rear reflector (h) being 90, 100, and 110 mm. The fine-tuning distances (L_4) from the ground plane to the reflector bottom edge are 5, 6, and 7 mm, and the radii (r_1) from 68, 78, and 88 mm.

Figure 4 illustrates that the optimal simulation parameters set for the reconstructed antenna are width (W_3) = 240 mm, length (L_3) = 240 mm, height (h) = 100 mm, length (L_4) = 5 mm, and radius (r_1) has also been increased to 78 mm. Simulation results for S_{11} were -11.18 dB at the low resonance frequency of 1.1 GHz (0.9861–1.301 GHz) and 25.09 dB at the high resonance frequency of 2.037 GHz (1.510–2.601 GHz). However,

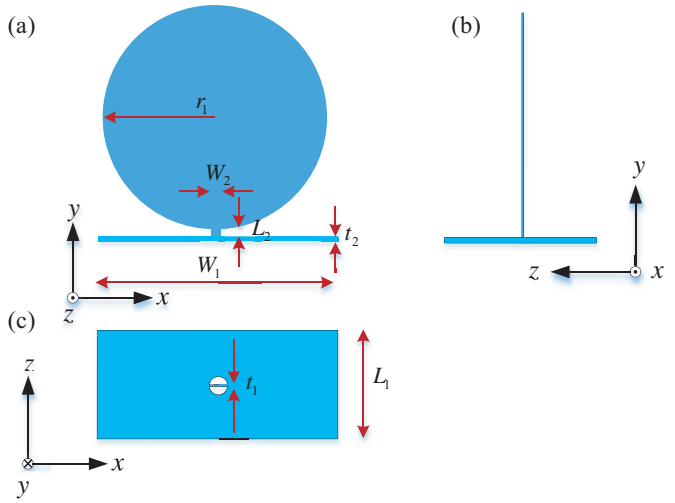

FIGURE 1. Elementary circular monopole antenna structure: (a) front view, (b) side view, and (c) bottom view.

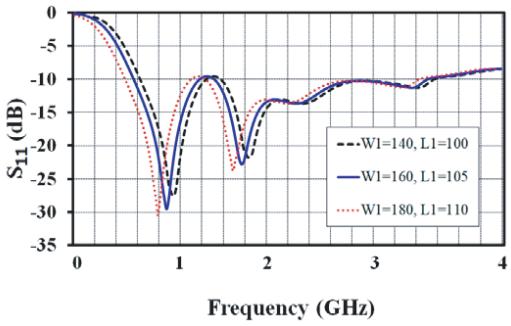

FIGURE 2. Reflection coefficient simulation results of the circular antenna in the first tuning step.

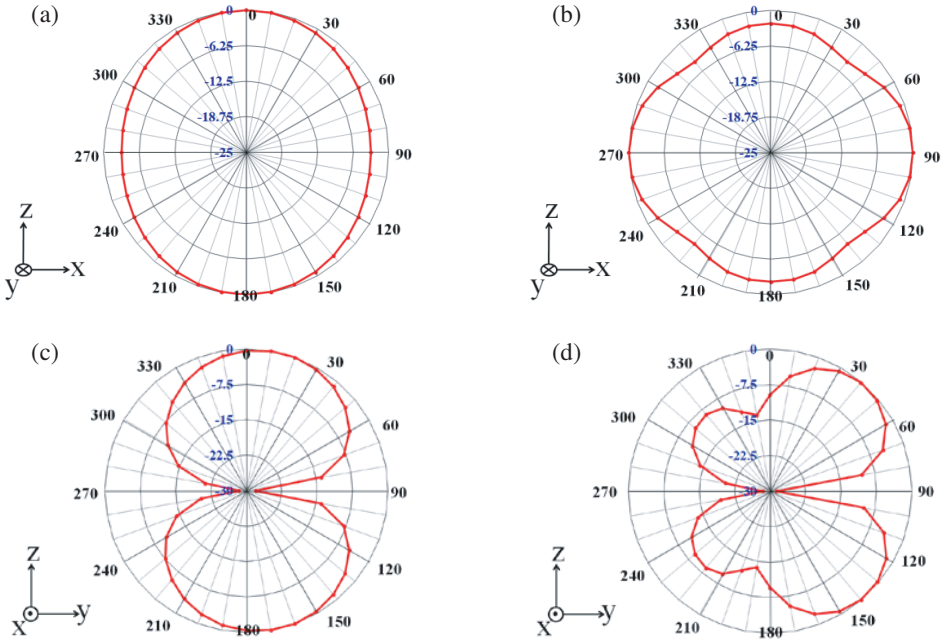

FIGURE 3. Radiation pattern simulation results of the circular antenna in the first tuning step: (a) at 900 MHz in the XZ-plane, (b) at 1.6 GHz in the XZ-plane, (c) at 900 MHz in the YZ-plane, and (d) at 1.6 GHz in the YZ-plane.

in the GSM-850 (0.80 to 0.90 GHz) and GSM-900 (0.88 to 0.96 GHz), S_{11} did not drop below -10 dB, and the frequency range did not cover the standard in the desired bandwidth. To encompass the standard operating frequency ranges of GSM-850 and GSM-900, the center of the frequency range in Figure 5 had to be shifted to the left side of the reflection coefficient graph. As depicted in Figure 6, the simulation results for the radiation pattern were unidirectional, with antenna gains of 8.27 dBi at 900 MHz and 8.51 dBi at 1.6 GHz.

In the third step, a rectangular slot was etched on the bottom left and right of the circular radiator using techniques in [23] and [24] that affected the shift of the resonance frequency to the lower frequency range. The rectangular slot had width (W_4) variations of 0.4, 0.5, and 0.6 mm, length (L_5) variations of 60, 65, and 70 mm distance d_1 variations of 25, 30, and 35 mm and distance d_2 variations of 25, 30, and 35 mm. It was found that $W_4 = 0.5$ mm, $L_5 = 65$ mm $d_1 = 30$ mm, and $d_2 = 30$ mm were the optimal values. The adaptation antenna structure of the third step is shown in Figure 7. The low resonant frequency at 0.852 GHz (0.686–0.947 GHz) had an S_{11} value of -26.46 dB, while the high resonance frequency at 1.707 GHz (1.476–2.603 GHz) had an S_{11} value of -19.07 dB, as shown in Figure 8, and the gains were 6.42 and 7.16 dBi, respectively. When considering the S_{11} simulation results, it was found that the operating frequency of the antenna did not cover the standard operating frequency of the WLAN of IEEE 802.11b/g/n

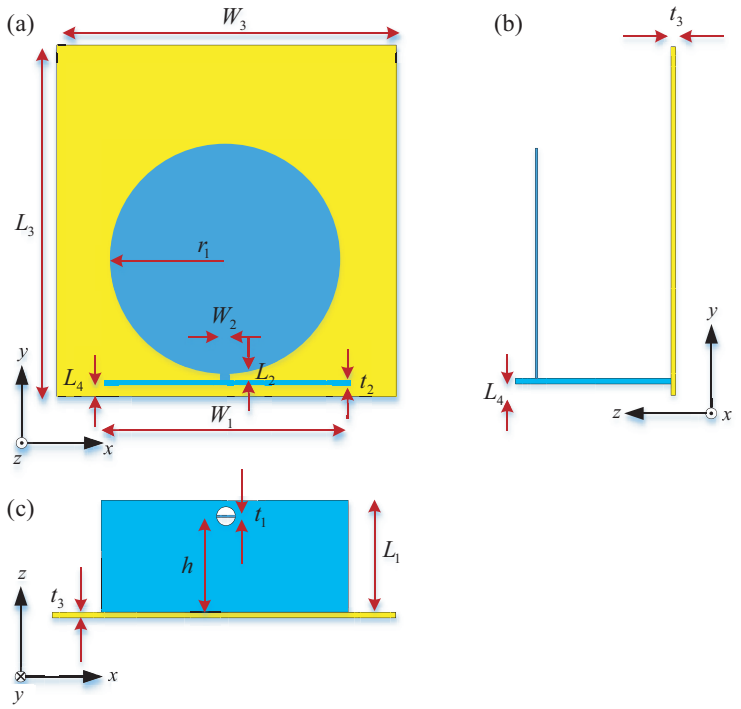

FIGURE 4. Reconstructed circular antenna structure (second tuning step) with rear reflector, (a) front view, (b) side view and (c) bottom view.

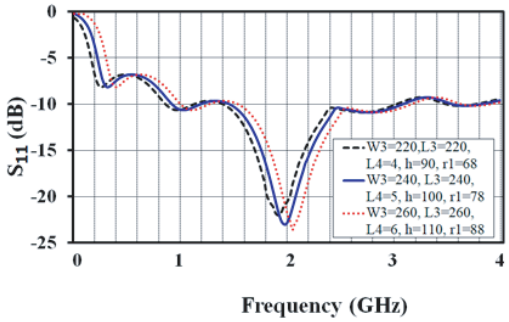

FIGURE 5. Reflection coefficient simulation results of the circular antenna in the second tuning step.

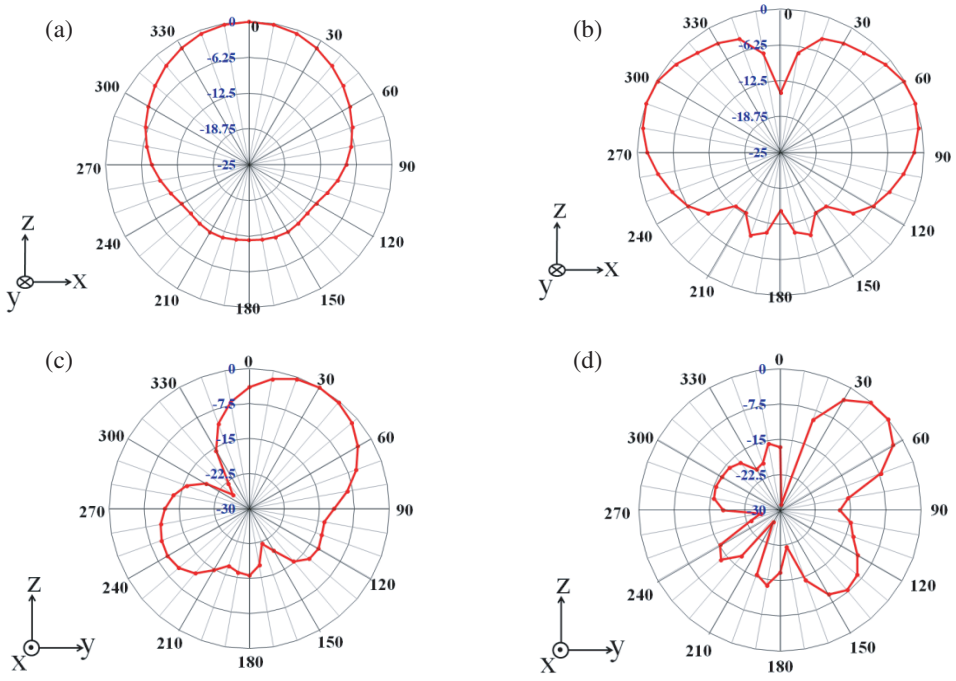

FIGURE 6. Radiation pattern of the circular antenna in the second tuning step: (a) at 900 MHz in the XZ-plane, (b) at 1.6 GHz in the XZ-plane, (c) at 900 MHz in the YZ-plane, and (d) at 1.6 GHz in the YZ-plane.

(2.4–2.48 GHz). Therefore, it is necessary to adjust the antenna structure to enhance the antenna properties and support the desired frequency range.

The final step of structure tuning consisted of cutting a bottom radiator section on both the left and right sides near the rectangular slots (done in the third step of tuning) to obtain resonance frequencies near 2.4 GHz [23, 24]. Width (W_5) adjustments of 21, 23, and 25 mm and length (L_6) adjustments of 14, 15, and 16 mm have been applied to the cutting sections of the circular radiator. The simulation results indicated that

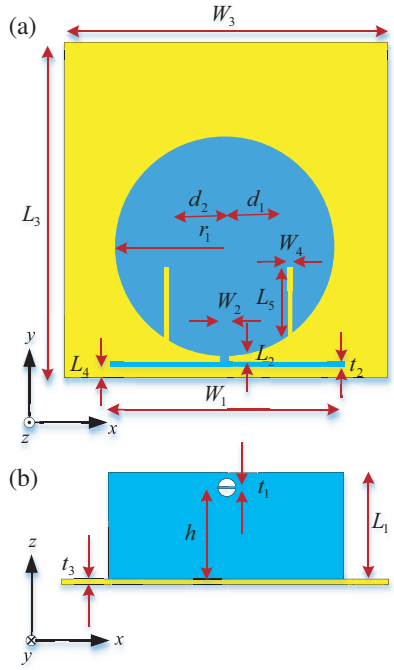

FIGURE 7. Reconstructed circular antenna structure (third tuning step) with dual rectangular slots (a) front view and (b) bottom view.

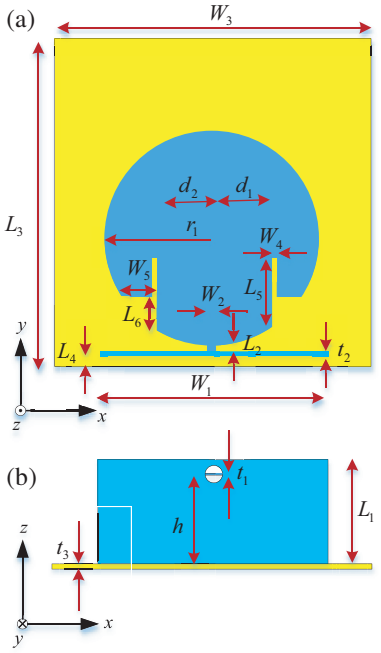

FIGURE 9. Reconstructed circular antenna structure (third tuning step) with dual rectangular slots (a) front view and (b) bottom view.

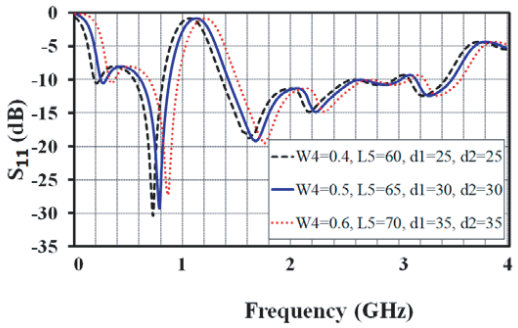

FIGURE 8. Reconstructed circular antenna structure (final tuning phase) with a cutting section of the radiator, (a) front and (b) bottom views.

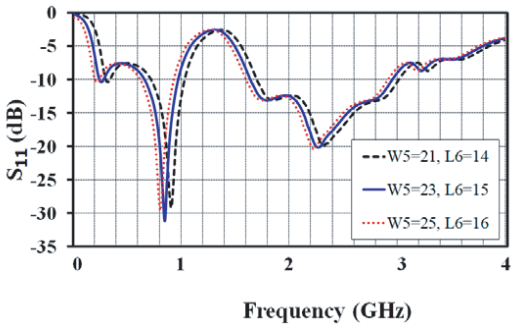

FIGURE 10. Reflection coefficient simulation results of the circular antenna in the final step (sea pimp shape) of tuning.

$W_5 = 23$ mm and $L_6 = 15$ mm were optimal dimensions. Figure 9 shows an overview of the completed antenna structure, which resembles a sea pimp shape.

Figure 10 displays S_{11} that were -20.15 dB at the high resonance frequency of 2.284 GHz (1.680–2.940 GHz) and -26.59 dB at the low resonance frequency of 0.915 GHz (0.736–1.040 GHz). The above frequency range covered applications for the following operating frequencies: GSM-850 (0.80–0.90 GHz), GSM-900 (0.88–0.96 GHz), DCS (1.72–1.88 GHz), PCS (1.85–1.99 GHz), UMTS (1.92–2.17 GHz), and WLAN IEEE 802.11b/g/n (2.4–2.48 GHz).

Figure 11 shows the results of the simulation according to the radiation pattern. The results indicate that the pattern tends to operate in the 0-degree direction in the XZ plane and that the pattern tends to be in the 30-degree direction in the YZ plane. Additionally, the gains were identified as 6.7 dBi at 900 MHz and 8.47 dBi at 2.28 GHz.

In terms of fine-tuning the antenna structure from the first to the last tuning step, it has resulted in changing the S_{11} value until it can support all desired frequencies. The best bandwidth at low frequency (BW_L) ranges from 0.736 to 1.040 GHz, with a low resonance frequency (f_{rL}) of 0.915 GHz. Conversely, the optimal bandwidth at high frequency (BW_H) spans from 1.680 to 2.940 GHz, with a high resonance frequency (f_{rH}) of 2.284 GHz. All variations can be seen in Figure 12 and Table 1. The final modified version of the proposed antenna is shown in Figure 13, which resembles a sea pimp and has the optimal parameters as detailed in Table 2.

3. FABRICATION AND MEASUREMENTS

3.1. Comparing Simulation and Measurement Results

The sea pimp-shaped monopole antenna, depicted in Figures 14(a)–(b), was manufactured utilizing the best simulation

TABLE 1. Bandwidth that results from each circular monopole antenna restructuring stage.

Step of design	BW_L (GHz)	f_{rL} (GHz)	BW_H (GHz)	f_{rH} (GHz)
1	0.639–1.236	0.914	1.368–3.302	1.617
2	0.986–1.301	1.100	1.510–2.600	2.037
3	0.686–0.947	0.852	1.476–2.603	1.717
4	0.736–1.040	0.915	1.680–2.940	2.284

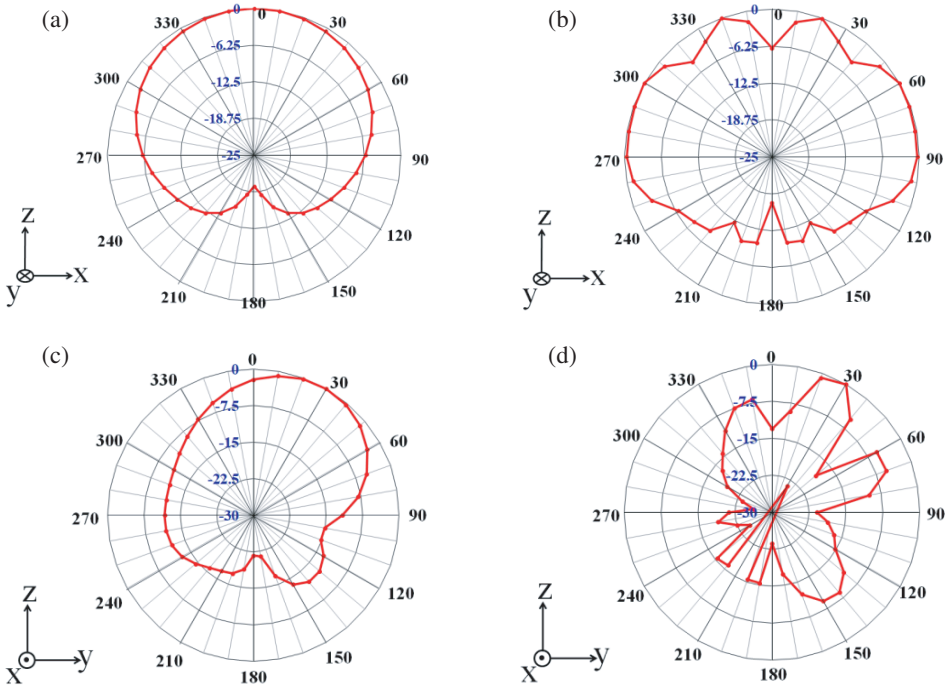

FIGURE 11. Radiation pattern of the proposed sea pimp-shaped antenna: (a) at 900 MHz in the XZ-plane, (b) at 2.28 GHz in the XZ-plane, (c) at 900 MHz in the YZ-plane, and (d) at 2.28 GHz in the YZ-plane.

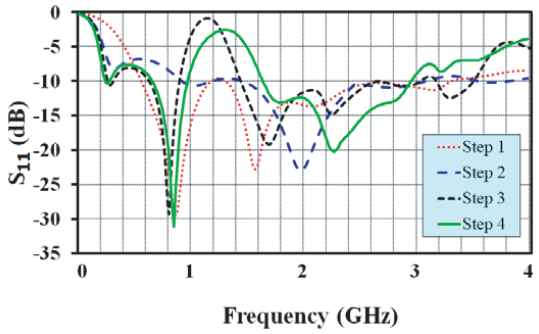

FIGURE 12. Reflection coefficient simulation results of the proposed circular monopole antenna with adjustments from the first to the final tuning process.

results derived from the optimal antenna structure parameters, as shown in Table 2. The radiator, reflector, and ground plane of the fabrication antenna were constructed separately from the galvanized metal sheet because it is abrasion-resistant, lightweight, and inexpensive. For assembling the three galvanized elements of the antenna, soldering method was used during the construction process. As the structure between the radiator and reflector has a large space, and the galvanized plate is flexible, plastic bolts were used to fasten and support the structure. For measurement results, various properties of the proposed antenna were measured using the Agilent network analyzer model E8363B in the chamber room, as depicted in Figure 14(c), and compared with simulation results in the frequency range of DC to 4 GHz, as shown in Figure 15.

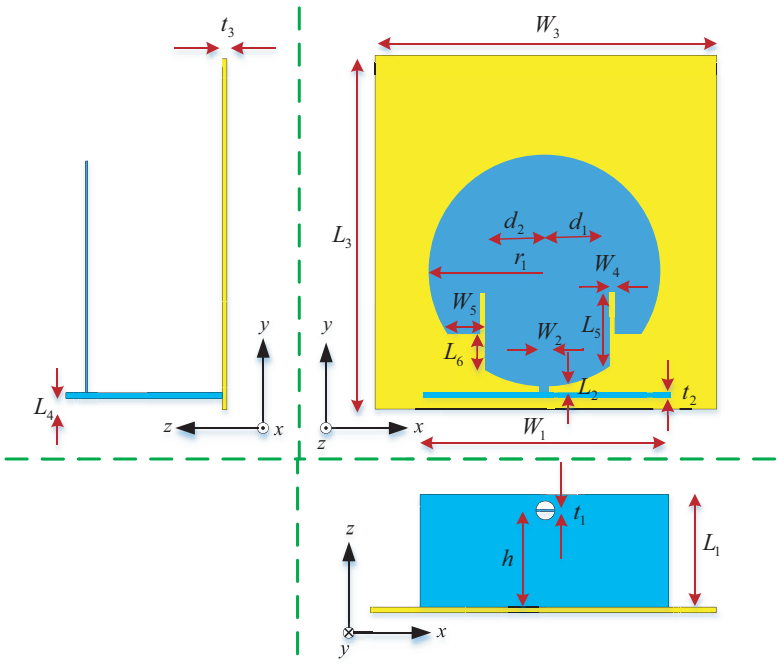

FIGURE 13. Sea pimp-shaped monopole antenna structure.

TABLE 2. Optimal parameters of the proposed sea pimpshaped monopole antenna.

Parameters	Size (mm)
r_1: radius of the radiator	78.0
d_1, d_2: distance from the center of antenna to the slot	30.0
W_1: width of the ground plane	160.0
W_2: width of fed	3.1
W_3: width of the reflector	240.0
W_4: width of the first slot	0.5
W_5: width of the second slot	23.0
L_1: length of the ground plane	105.0
L_2: length of fed	4.0
L_3: length of the reflector	240.0
L_4: gap of the ground plane on the reflector	5.0
L_5: length of the first slot	65.0
L_6: length of the second slot	15.0
t_1: thickness of the radiator	0.3
t_2: thickness of the ground plane	0.3
t_3: thickness of the reflector	0.3
h: height of the radiator on the reflector	100.0

The results of the measurements showed a trend in the same direction as the results of the simulation.

Table 3 presents the data regarding the reflection coefficient obtained from both the simulated and measured antennas at frequencies of 900 MHz and 2.45 GHz. The bandwidth values obtained from simulation and measurement at a frequency of 900 MHz are roughly 304 and 255 MHz, respectively. However, at a frequency of 2.45 GHz, the bandwidth values from simulation and measurement are 1260 and 1235 MHz, respectively. It is readily apparent that the bandwidth exhibits a greater width at higher frequencies than lower frequencies.

To evaluate the proposed antenna radiation pattern, the measurement equipment depicted in Figure 14(c) was set up within the chamber room. Figures 16 and 17 present the measurement and illustrate the results of the radiation pattern in the XZ and YZ planes, respectively, at frequencies of 0.90 and 2.45 GHz. The results indicate that the observed measurements indicate a similar pattern to the simulation results. The antenna sends out the most power at resonance frequencies of 0.90 and 2.45 GHz, which is at a 30° angle to the forward direction (along the z-axis) in the XZ and YZ planes.

Figure 18 shows the comparison of antenna gain, specifically the average gain obtained from both measured and simulation results, within the frequency range of 0.70 to 3.00 GHz. At a relatively low frequency, the gain exhibited its minimum value of approximately 5.35 dBi, while the maximum gain was observed at a high frequency, reaching a value of 8.98 dBi. This observation generally agrees with the simulation results.

3.2. Experimental Test

In this section, the outdoor antenna under test (AUT) application was set up as follows: The prototype antenna was installed in the plastic housing as shown in Figure 19(a), and the test equipment set was placed on the roof at a height from the ground about 4 meters, with about 200 meters from the mobile phone base station as shown in Figure 19(b). The Anritsu MS2713E spectrum analyzer was used to measure the receiving signal from the AUT. The test experiment was car-

TABLE 3. Comparison of reflection coefficient results from measurement and simulation of the proposed antenna at 900 MHz and 2.45 GHz.

Frequency (GHz)	Simulation			Measurement		
	Bandwidth (MHz)	f_r (MHz)	S_{11} (dB)	Bandwidth (MHz)	f_r (MHz)	S_{11} (dB)
0.900	0.736–1.040	0.915	−26.59	0.766–1.021	0.942	−29.30
2.450	1.680–2.940	2.228	−20.15	1.687–2.922	2.156	−18.62

FIGURE 14. Providing the ability to measure reflection coefficient and radiation patterns: (a) the front view of the antenna prototype, (b) the antenna prototype in its housing, and (c) setting up the network analyzer and antenna prototype in the chamber room.

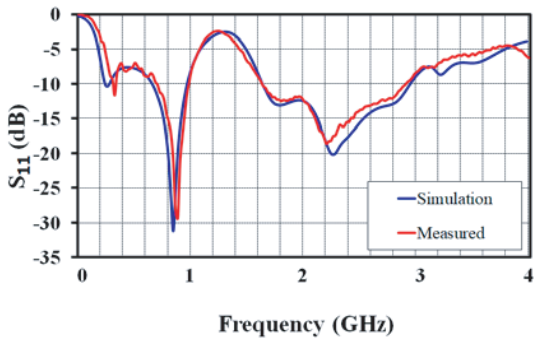

FIGURE 15. Reflection coefficient comparisons of simulation and measurement results for the proposed sea pimp-shaped antenna.

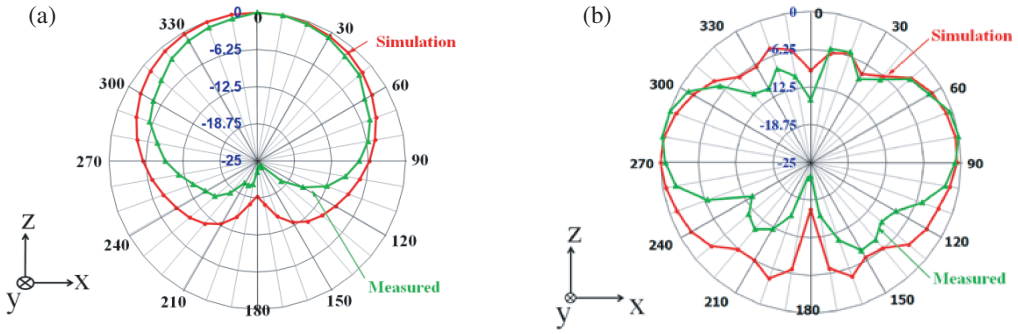

FIGURE 16. Comparison of measurement and simulation results in the radiation pattern in the XZ-plane: (a) at 0.90 GHz and (b) at 2.45 GHz.

ried out at the mobile phone base station of DTAC Company, the Chao Pluk Node, Chao Pluk subdistrict, Maharat district, Phranakhon Si Ayutthaya province, Thailand, with coordinates of latitude 14°35′19.03″ North and longitude 100°32′6.36″ East. The prototype antenna could receive five frequency channels at 769.00 MHz (−50.28 dB), 880.00 MHz (−48.76 dB), 956.00 MHz (−45.86 dB), 1.816 GHz (−46.67 dB), and 2.137 GHz (−44.02 dB), as shown in Figure 19(c). The measurement results confirmed that the proposed antenna can transmit and receive signals following mobile 4G/5G/LTE41 standards.

The AUT applies to the internet system via Wi-Fi during case-experimental testing. The device used for testing is a ZTE (model: ZXHN 6107) access point router. The displacement

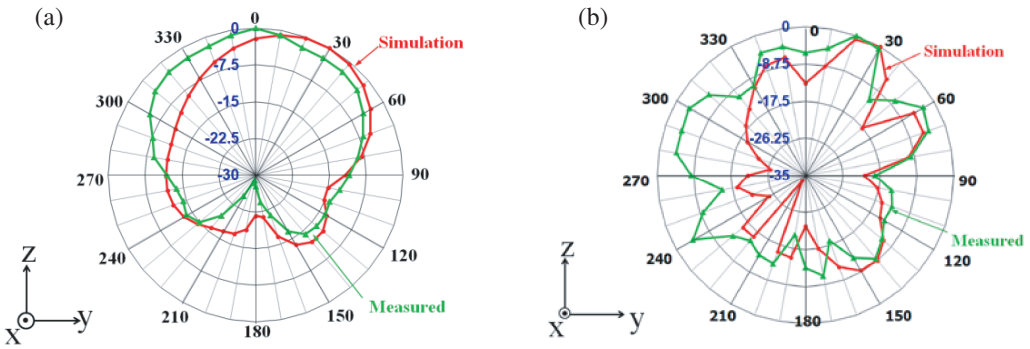

FIGURE 17. Comparison of measurement and simulation results in the radiation pattern in the YZ-plane: (a) at 0.90 GHz and (b) at 2.45 GHz.

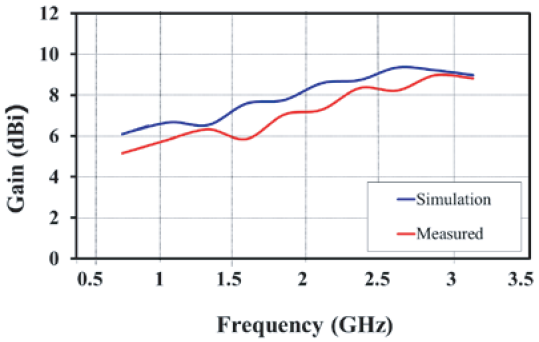

FIGURE 18. Comparison of measurement and simulation average gain in the frequency range from 700 MHz to 3 GHz.

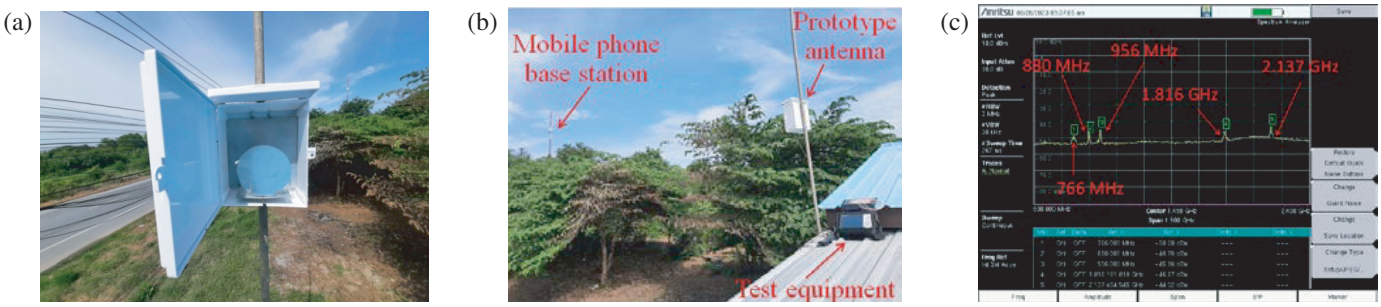

FIGURE 19. Preparing experiments for mobile signals, (a) the prototype antenna was in a plastic box, (b) a set of test equipment, and (c) the receiving signal was at a spectrum analyzer.

between the access point router (AP router) location and the AUT is approximately 40 meters, as depicted in Figure 20(a). The internet signal was then transmitted through the AP router to evaluate the Wi-Fi receiving performance of the AUT. The results of the measurements indicate that the presented antenna can receive Wi-Fi signals on channel 8 at 2.447 GHz exceptionally well. As depicted in Figure 20(b), the average signal level received from the antenna was -44.96 dB.

4. DISCUSSION

The comparative analysis of the prototype antenna was carried out concerning various circular monopole antennas, as shown in Table 4. The design of the circular monopole antenna [16] involved using copper material on an FR4 substrate. This antenna was explicitly designed to operate within the frequency range of 2.69–10.60 GHz while exhibiting a gain ranging from 3.5–6.7 dBi. As described in [17], the circular antenna was constructed using a metallic material on a very big ground plane to facilitate its operation over the frequency range of 0.40–4.00 GHz. The antenna indicated a gain that ranged from 5 to 8 dBi. The elliptical monopole antenna [20] was developed using copper material on an FR4-printed circuit board. This design was intended to enable the antenna to operate in two frequency bands: 1.69–3.15 and 4.93–6.62 GHz. The antenna exhibited gains of 3.1 and 5.1 dBi in these respective frequency ranges. The gains of a circular monopole antenna [21] constructed using an FR4-printed circuit board for dual-band applications inside the 0.82–1.25 and 1.65–2.79 GHz frequency ranges were measured to be 3.7 dBi. The design of a circular

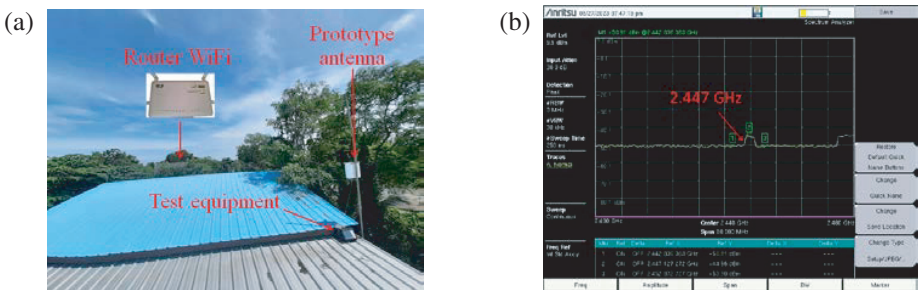

FIGURE 20. Preparing experimental WLAN, (a) the prototype antenna and test equipment set, and (b) receiving the signal from a spectrum analyzer at 2.452 GHz.

TABLE 4. The summary descriptions for the comparative antennas.

Reference	Material	Radius of antenna (mm)	Ground plane (mm)	Bandwidth (GHz)	Average gain (dBi)
[16]	FR4	10.0	42×50	2.69–10.60	3.5–6.7
[17]	Metal sheet	85.0	300×300	0.40–4.00	5.0–8.0
[20]	FR4	24.1	$r = 61.2$	1.69–3.15 and 4.93-6.62	3.1 and 5.1
[21]	FR4	50.0	50×100	0.82–1.25 and 1.65–2.79	3.7
[22]	FR4	12.0	16×40	1.48–35.00	0.0–5.25
[29]	Metal sheet	25.0	300×300	1.21–13.00	4.0–7.0
The proposed antenna	Galvanized metal sheet	78.0	105×160	0.736–1.040 and 1.680–2.940	6.7 and 8.47

monopole antenna [22] was implemented using an FR4 printed circuit board to enable the UWB frequency, spanning from 1.48 to 35.00 GHz. This antenna configuration yielded a gain ranging from 0 to 5.25 dBi. The circular disc monopole antenna [29] was constructed using a metal sheet to facilitate a broad frequency range of 1.17–12.00 GHz, resulting in a gain of 4–7 dBi. The prototype antenna was constructed using a galvanized metal sheet on a medium ground plane that possesses an elementary structure, is easily accessible, simple to assemble, inexpensive, covering 0.736–1.040 GHz and 1.680–2.940 GHz, and exhibits enhanced gains of 6.7 and 8.47 dBi in comparison to the average gains in Table 4, about two to three times greater at the same frequency.

5. CONCLUSION

The monopole antenna structure, resembling the sea pimp shape, was designed through the utilization of etching techniques and the incorporation of reflectors. This made it possible to shift the frequency range to cover both cellular and WLAN bandwidth according to the standards GSM-850 (0.82–0.90 GHz), GSM-900 (0.88–0.96 GHz), DCS (1.72–1.88 GHz), PCS (1.85–1.99 GHz), UMTS (1.92–2.17 GHz), 5G band 40 (2.30–2.40 GHz), LTE41 (2.496–2.690 GHz), and WLAN band IEEE 802.11b/g/n (2.4–2.48 GHz). The simulation results regarding the reflective coefficient were -26.70 and -20.15 dB for the low resonance frequency of 915 MHz (with a frequency range of 736–1040 MHz) and the high resonance frequency of 2.28 GHz (with a frequency range of 1.68–2.94 GHz), respectively. The antenna gain results were obtained at 6.70 and 8.47 dBi, respectively. These values represent an increase of 83.56 and 44.04% compared to the initial design without a reflector. Additionally, the antenna indicated a unidirectional pattern which allowed for more energy to be received and could be used for future RF energy-harvesting (RF-EH) systems. The measured results exhibited a significant level of agreement with the simulated ones. The prototype antenna structure has multiple important advantages, including its ease of design, utilization of cost-effective materials, and resistance to rusting. Furthermore, the prototype has a response in terms of frequency coverage and gain, surpassing traditional antennas operating at the same frequency.

ACKNOWLEDGEMENT

The authors would like to thank the Department of Telecommunications Engineering, Faculty of Engineering and Technology, Rajamangala University of Technology Isan, for providing the equipment. The authors also gratefully acknowledge the Department of Electronics and Telecommunication Engineering, Faculty of Engineering, Rajamangala University of Technology Thanyaburi, Pathum Thani, for supporting this work with

the simulation CST software, and the Department of Electrical Engineering, Faculty of Engineering and Architecture, Rajamangala University of Technology Suvarnabhumi, Phranakhon Si Ayutthaya, for supporting the experimental site.

REFERENCES

[1] Takamura, H., A. Nakajima, and K. Yamamoto, "Network and signaling structure based on personal digital cellular telecommunication system concept," in *IEEE 43rd Vehicular Technology Conference*, 922–926, 1993.

[2] Wang, J. C. and B. Hsu, "On the analysis of a cellular mobile telecommunication electrical power system," in *2004 IEEE International Conference on Electric Utility Deregulation, Restructuring and Power Technologies Proceedings*, Vol. 2, 535–539, 2004.

[3] Saeed, R. A., A. B. H. Naemat, A. B. Aris, and M. K. B. Awang, "Design and evaluation of lightweight IEEE 802.11 p-based TDMA MAC method for road side-to-vehicle communications," in *2010 The 12th International Conference on Advanced Communication Technology (ICACT)*, Vol. 2, 1483–1488, 2010.

[4] Tang, X.-G. and Z. Ding, "Low-complexity iterative equalization for EDGE with bidirectional processing," *IEEE Transactions on Wireless Communications*, Vol. 4, No. 5, 1963–1968, 2005.

[5] Kim, Y.-J., S.-S. Nam, and H.-M. Lee, "Frequency selective surface superstrate for wideband code division multiple access system," in *2009 European Wireless Technology Conference*, 33–36, 2009.

[6] Ko, H., G. Lee, D. Suh, S. Pack, and X. Shen, "An optimized and distributed data packet forwarding scheme in LTE/LTE-A networks," *IEEE Transactions on Vehicular Technology*, Vol. 65, No. 5, 3462–3473, 2015.

[7] Andrade, de T. P. C., C. A. Astudillo, and N. L. D. Fonseca, "Allocation of control resources for machine-to-machine and human-to-human communications over LTE/LTE-A networks," *IEEE Internet of Things Journal*, Vol. 3, No. 3, 366–377, 2016.

[8] Cao, J., M. Ma, H. Li, Y. Zhang, and Z. Luo, "A survey on security aspects for LTE and LTE-A networks," *IEEE Communications Surveys & Tutorials*, Vol. 16, No. 1, 283–302, 2013.

[9] Awwad, M., N. Rafaiah, and O. A. Saraereh, "Design of mimo antenna array for 5G smart phone applications operating in LTE bands," in *2019 8th Asia-Pacific Conference on Antennas and Propagation (APCAP)*, 1–2, 2019.

[10] Karli, R. and H. Ammor, "A simple and original design of multiband microstrip patch antenna for wireless communication," *International Journal of Microwaves Applications*, Vol. 2, No. 4, 1303–1306, 2013.

[11] Malek, M. A., S. Hakimi, S. K. A. Rahim, and A. K. Evizal, "Dual-band CPW-fed transparent antenna for active RFID tags," *IEEE Antennas and Wireless Propagation Letters*, Vol. 14, 919–922, 2014.

[12] Li, L., X. Zhang, X. Yin, and L. Zhou, "A compact triple-band printed monopole antenna for WLAN/WiMAX applications," *IEEE Antennas and Wireless Propagation Letters*, Vol. 15, 1853–1855, 2016.

[13] Chanramrd, S., W. Naktong, P. Thongbor, S. Sakulchat, A. Ruengwaree, and A. Namsang, "The structure tuning of plugs-shaped monopole antenna for wireless communication applications," in *2017 International Symposium on Antennas and Propagation (ISAP)*, 1–2, 2017.

[14] Kim, W.-S. and J.-H. Yoon, "A design for a CPW-fed monopole antenna with two modified half circular rings for WLAN/WiMAX operations," *Journal of Information and Communication Convergence Engineering*, Vol. 13, No. 3, 159–166, 2015.

[15] Kornsing, S., A. Innok, W. Naktong, and A. Ruengwaree, "The ring antenna with circular probe feeding for MIMO systems," in *2017 International Symposium on Antennas and Propagation (ISAP)*, 1–2, 2017.

[16] Liang, J., C. C. Chiau, X. Chen, and C. G. Parini, "Study of a printed circular disc monopole antenna for UWB systems," *IEEE Transactions on Antennas and Propagation*, Vol. 53, No. 11, 3500–3504, 2005.

[17] Qiu, J. and J. Qi, "Study on the properties of circular monopole antenna," in *2006 6th International Conference on ITS Telecommunications*, 422–425, 2006.

[18] Powell, J. and A. Chandrakasan, "Spiral slot patch antenna and circular disc monopole antenna for 3.1–10.6 GHz ultra wideband communication," *ISAP 2004*, Vol. 8, 1–10, 2004.

[19] Zhong, L. L., J. H. Qiu, N. Zhang, and B. Zhao, "Novel ultrawide-band wide beam circular polarization antenna," in *Asia Pacific Microwave Conference (APMC)*, 1–4, 2007.

[20] Khoomwong, E. and C. Phongcharoenpanich, "Characteristics of a dual-broadband antenna with crossed elliptical probes and L-shaped slits," in *2017 International Symposium on Antennas and Propagation (ISAP)*, 1–2, 2017.

[21] Mardikar, A., R. Mohan, M. Arrawatia, and G. Kumar, "Dual band dual circular ring monopole antenna," in *2015 Twenty First National Conference on Communications (NCC)*, 1–5, 2015.

[22] Kumar, N., K. K. Singh, and R. K. Badhai, "A tapered feed circular monopole super ultra-wideband (UWB) printed antenna," in *2016 International Conference on Communication and Signal Processing (ICCSP)*, 1943–1946, 2016.

[23] Ruengwaree, A., W. Naktong, and A. Namsang, "A TE-shaped monopole antenna with semicircle etching technique on ground plane for UWB applications," in *2013 Proceedings of The International Symposium on Antennas & Propagation*, Vol. 1, 95–98, 2013.

[24] Naktong, W., A. Ruengwaree, and P. Tajchai, "A study of tuning the CPW fed basic geometric monopole antenna for UWB applications," *Naresuan University Engineering Journal*, Vol. 15, 17–32, 2020.

[25] Dash, S. K. K. and T. Khan, "Reflector backed conical dielectric resonator antenna with enhanced gain," in *2018 IEEE Indian Conference on Antennas and Propogation (InCAP)*, 1–3, 2018.

[26] Ranga, Y., L. Matekovits, K. P. Esselle, and A. R. Weily, "Enhanced gain UWB slot antenna with multilayer frequency-selective surface reflector," in *2011 International Workshop on Antenna Technology (iWAT)*, 176–179, 2011.

[27] Prakash, P., M. P. Abegaonkar, A. Basu, and S. K. Koul, "Gain enhancement of a CPW-fed monopole antenna using polarization-insensitive AMC structure," *IEEE Antennas and Wireless Propagation Letters*, Vol. 12, 1315–1318, 2013.

[28] Naktong, W., B. Piyadanai, T. Patsakul, and A. Ruengwaree, "A Study of the placement of the ring antenna with circular-shaped probe feeding for MIMO system application," *EENET Journal*, Vol. 1, No. 2, 1–4, 2017.

[29] Agrawall, N. P., G. Kumar, and K. P. Ray, "Wide-band planar monopole antennas," *IEEE Transactions on Antennas and Propagation*, Vol. 46, No. 2, 294–295, 1998.